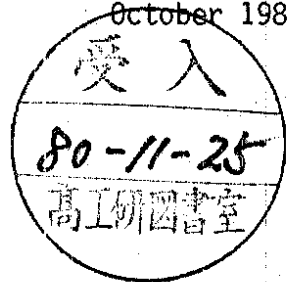


DESY 80/94  
October 1980



INELASTIC ELECTRON PHOTON SCATTERING AT MODERATE

FOUR MOMENTUM TRANSFERS

by

*PLUTO COLLABORATION*

DESY behält sich alle Rechte für den Fall der Schutzrechtserteilung und für die wirtschaftliche Verwertung der in diesem Bericht enthaltenen Informationen vor.

DESY reserves all rights for commercial use of information included in this report, especially in case of apply for or grant of patents.

To be sure that your preprints are promptly included in the  
HIGH ENERGY PHYSICS INDEX ,  
send them to the following address ( if possible by air mail ) :

DESY  
Bibliothek  
Notkestrasse 85  
2 Hamburg 52  
Germany

INELASTIC ELECTRON PHOTON SCATTERING AT MODERATE  
FOUR MOMENTUM TRANSFERS

BY

PLUTO COLLABORATION

Ch.Berger, H.Genzel, R.Grigull, W.Lackas, F.Raupach  
I. Phys. Institut der RWTH Aachen <sup>1</sup>, Germany,

A.Klovning, E.Lillestøl, J.A.Skard,  
University of Bergen <sup>2</sup>, Norway,

H.Ackermann, J.Bürger, L.Criegee, H.C.Dehne, A.Eskreys<sup>3</sup>, G.Franke,  
W.Gabriel<sup>4</sup>, Ch.Gerke, G.Knies, E.Lehmann, H.D.Mertiens, U.Michelsen,  
K.H.Pape, H.D.Reich, M.Scarr<sup>5</sup>, B.Stella<sup>6</sup>, U.Timm, W.Wagner,  
P.Waloschek, G.G.Winter, W.Zimmermann,  
Deutsches Elektronen Synchrotron DESY, Hamburg, Germany,

O.Achterberg, V.Blobel<sup>7</sup>, L.Boesten, V.Hepp<sup>8</sup>, H.Kapitza, B.Koppitz,  
B.Lewendel, W.Lührsen, R.van Staa, H.Spitzer,  
II. Institut für Experimentalphysik der Universität Hamburg <sup>1</sup>, Germany,

C.Y.Chang, R.G.Glasser, R.G.Kellogg, K.H.Lau, R.O.Polvado,  
B.Sechi-Zorn, A.Skuja, G.Welch, G.T.Zorn,  
University of Maryland <sup>9</sup>, USA

A.Bäcker<sup>10</sup>, F.Barreiro, S.Brandt, K.Derikum, C.Grupen, H.J.Meyer,  
B.Neumann, M.Rost, G.Zech,  
Gesamthochschule Siegen <sup>1</sup>, Germany,

H.J.Daum, H.Meyer, O.Meyer, M.Rössler, D.Schmidt,  
Gesamthochschule Wuppertal <sup>1</sup>, Germany

(Submitted to Phys. Lett.)

- <sup>1</sup> Supported by the BMFT, Germany
- <sup>2</sup> Partially supported by the Norwegian Council for Science  
and Humanities
- <sup>3</sup> Now at Institute of Nucl. Physics, Krakow, Poland
- <sup>4</sup> Now at Max Plank Institut für Limnologie, Plön, Germany
- <sup>5</sup> On leave from University of Glasgow, Scotland
- <sup>6</sup> On leave from University of Rome, Italy; partially supported by INFN
- <sup>7</sup> Now at CERN, Geneva, Switzerland
- <sup>8</sup> Now at Heidelberg University, Germany
- <sup>9</sup> Partially supported by Dept. of Energy, USA
- <sup>10</sup> Now at Harvard University, USA

## Abstract

We present new high statistics data on hadron production in photon photon reactions. The data are analyzed in terms of an electron photon scattering formalism. The dependence of the total cross section on  $Q^2$ , the four momentum transfer squared of the scattered electron, and on the mass  $W$  of the hadronic system is investigated. The data are compared to predictions from Vector Meson Dominance and the quark model.

High energy electron positron storage rings offer the opportunity to measure the inclusive reaction  $e^+e^- \rightarrow e^+e^- + \text{hadrons}$ . These reactions are usually interpreted as hadron production by two virtual photons which are radiated from the incoming leptons ( $e^+e^- \rightarrow e^+e^- \gamma^* \gamma^* \rightarrow e^+e^- + \text{hadrons}$ ). Experimentally these reactions can be easily separated from the annihilation processes ( $e^+e^- \rightarrow \gamma^* \rightarrow \text{hadrons}$ ) by detecting one of the outgoing leptons at small angles in the forward direction ('single tagging'). If on the other hand the scattering angle of the second lepton is kept very small by excluding events with an angle greater than e.g. 25 mrad ('antitagging'), the radiated photon is practically on mass shell and purely transverse polarized. This is the kinematical situation of electron scattering (lepton 1 in fig. 1) off a real photon beam.

The inclusive cross section for this process ( $e\gamma \rightarrow eX$ ) is given by

$$d\sigma(e\gamma \rightarrow eX) = \Gamma_t [\sigma_t(Q^2, W) + \varepsilon \sigma_l(Q^2, W)] d\Omega_1 dE'_1 \quad (1)$$

The kinematical quantities are explained in fig.1.  $\Gamma_t$  is the flux factor for the incoming virtual photons radiated from lepton 1 and  $\varepsilon$  is a polarization parameter for the virtual photons.  $\sigma_t$  is the total cross section for the scattering of virtual transverse polarized photons off real photons and  $\sigma_l$  the respective cross section for virtual longitudinal photons.  $\Gamma_t$  and  $\varepsilon$  are respectively given by

$$\Gamma_t = \frac{\alpha E'_1 (1 + (1-y)^2)}{2\pi^2 Q^2 y} \quad (2)$$

$$\varepsilon = 2(1-y)/(1+(1-y)^2)$$

$$\text{with } y = 1 - (E'_1/E) \cos^2(\Theta_1/2) \quad (3)$$

as a measure for the relative energy of the virtual photon.

The inclusive cross section for the reaction  $e^+e^- \rightarrow e^+e^- + \text{hadrons}$  is then given by

$$\sigma(e^+e^- \rightarrow e^+e^- + \text{hadrons}) = d\sigma(e\gamma \rightarrow eX) N(z, \Theta_{2\max}) dz \quad (4)$$

$N(z, \Theta_{2\max}) dz$  is the number of incoming quasireal photons in the energy interval  $dz$  ( $z = E_\gamma/E$  radiated from leptons with a maximum scattering angle  $\Theta_{2\max}$ ). A standard expression is given by<sup>1,2</sup>

$$N(z, \Theta_{2\max}) = \alpha/(\pi z) \left( (1 + (1-z)^2) \ln[(E/m)((1-z)/z)\Theta_{2\max}] - 1 + z \right) \quad (5)$$

A similar formula published in the literature<sup>3</sup> produces numerical differences of less than 5 % for the experimental conditions accessible to our detector. The cross section definition for photon photon reactions ( $\sigma_t, \sigma_l$ ) agrees with ref. 1 and leads to the above expressions for  $\Gamma_t$  and  $\varepsilon$  which slightly differ from those given in our first paper<sup>4</sup>, but do not contain any small angle approximations.  $\Gamma_t N$  exactly reproduces the single tag luminosity function given in formula 11 of ref. 5.

In our previous publication<sup>4</sup> we presented cross section measurements up to  $W$  values of 6.5 GeV at a  $\langle Q^2 \rangle$  of 0.1 GeV<sup>2</sup>. Our new data extend this

range up to  $W=8.5\text{GeV}$  and  $Q^2=0.6\text{ GeV}^2$ . The much higher number of events allows for a detailed study of the  $W$  and  $Q^2$  dependence.

The experiment has been performed using the detector PLUTO at PETRA the  $e^+e^-$  colliding beam machine at DESY. A description of the experimental set up can be found in refs. 4 and 6. The data reported in this paper have been taken at beam energies between 15 and 16 GeV ( $\langle E \rangle = 15.5\text{ GeV}$ ) for an integrated luminosity of  $2700\text{ nb}^{-1}$  as determined by the luminosity monitor.

Hadronic events from electron photon scattering have been defined by the following conditions:

a) a tag signal on one side, i.e. we have requested a deposited energy of more than 4 GeV in one of the small angle taggers (SAT) of the forward spectrometers ( $23\text{mrad} < \theta_1 < 55\text{mrad}$ ).

b) 'antitagging' on the opposite side, i.e. events with a tag signal in any part of the opposite side forward spectrometer (small angle tagger and large angle tagger) have been rejected, thus keeping  $\theta_{2\text{max}} < 23\text{ mrad}$ .

c) three or more tracks in the central detector or 2 tracks in the central detector and at least one shower which is not associated with the tracks ( $E_n > 150\text{MeV}$ ,  $|\cos\theta_n| < .966$ ). The two tracks have been defined by the following conditions:  $|\cos\theta_{h1}| < 0.629$ ,  $p_T > 350\text{MeV}$ ,  $|\cos\theta_{h2}| < .866$ ,  $p_T > 100\text{ MeV}$ , where  $p_T$  is the transverse momentum,  $\theta_n$  and  $\theta_{hi}$  are the polar angles of showers and hadrons relative to the beam axis. Two of the tracks in multitrack events are subject to the same conditions.

After applying these cuts the contamination from beam gas scattering was approximately 15%. Using the vertex position along the beam this background has been subtracted on a statistical basis. The resulting number of events after all cuts is  $488 \pm 27$ .

The total cross sections  $\sigma_t$  and  $\sigma_1$  depend on  $Q^2$ , the mass squared of the virtual photon, and on  $W$ , the invariant mass of the hadronic system.  $Q^2$  has been determined from the energy and angle of the scattered lepton as measured in the SAT. Due to the fine granularity and the good energy resolution of the system the error in the determination of  $Q^2$  is rather small, typically 15%. The invariant mass  $W$  of the hadronic system has been determined from the showers and tracks in the central detector assuming pion masses for all charged particles. Because of particle losses (due to the limited acceptance of our detector, reconstruction losses etc.) the visible invariant mass  $W_{\text{vis}}$  is always lower than the true mass, typically by 15–20 %. Our conclusions do not depend critically on the difference between  $W$  and  $W_{\text{vis}}$  and thus an unfolding procedure has only been applied in the final step of the analysis (see below).

We have calculated the detection efficiency via a Monte Carlo program simulating the electron photon scattering process in the PLUTO detector. The angle and energy spectra of the outgoing leptons have been generated according to the formalism discussed above (formula 2 and 5). For the hadronic part of the cross section ( $\sigma_t + \epsilon\sigma_1$ ) we have used a multipion phase space model with limited transverse momentum (as familiar from other high energy hadronic scattering processes) and con-

stant production rate, independent of  $Q^2$  and  $W$ . Note, that the polarization parameter is practically constant ( $\varepsilon \sim 0.95$ ) in the kinematical range discussed in this paper, and it is thus impossible to separate  $\sigma_t$  from  $\sigma_1$ .

The detection efficiency has been found to depend critically on the transverse momentum cutoff. The inclusive  $p_T$  distribution for all our events is shown in fig.2. A single exponential does not fit the data. They are well reproduced however if 75 % of the events are generated according to  $\exp(-5p_T^2)$  and 25 % according to  $\exp(-1p_T^2)$  (solid line in fig.2). The charged multiplicity has been taken from low energy  $e^+e^-$  annihilation data<sup>7,8,9</sup> (parametrized by  $n=2+0.7\ln W^2$ ) and the ratio of charged pions to neutral pions has been taken as 2:1. The observed charged multiplicity and the observed number of showers is well consistent with the predictions from the Monte Carlo simulation.

The resulting cross section is plotted in fig. 3 versus  $W_{vis}$ , the visible invariant mass. Fig. 4a contains  $\sigma_t + \varepsilon\sigma_1$  as function of  $Q^2$  for  $W_{vis} < 3.5$  GeV whereas in fig 4b. we show the same quantity for  $W_{vis} > 3.5$  GeV. The figure 4a also contains the result from ref. 4 ( $\langle Q^2 \rangle = 0.1$  GeV<sup>2</sup>) measured at much smaller beam energies ( $\langle E \rangle = 7.8$  GeV). The errors given are statistical only, we estimate an additional overall normalization error of 20% mainly due to uncertainties in the hadronic cross section model. It must be noted that in contrast to the annihilation channel the probability for the detection of two photon initiated hadronic events is only in the order of 25% (not accounting for the tagging efficiency).

The  $W$  dependence of the data is relatively smooth, the cross section being practically constant above  $W_{vis} = 3$  GeV and increasing by a factor of 2-3 towards the smallest value of  $W_{vis}$ . It is quite obvious that the cross section drops with growing  $Q^2$ .

For the following discussion we put  $\sigma_1 = 0$  in accordance with the experience from electroproduction on hadronic targets. A rather flat  $W$  dependence can be calculated from theories applying the usual tools of hadronic physics, specifically resonance-Regge duality and factorization. A 'standard prediction' for  $\sigma_t(0, W)$  is<sup>10</sup>

$$\sigma_{\gamma\gamma}(W) = \sigma_t(0, W) = 240\text{nb} + 270\text{nbGeV}/W \quad (6)$$

As a first guess one would assume the  $Q^2$  dependence of the cross section to be given by the  $\rho$  pole form factor

$$\sigma_t(Q^2, W) = \sigma_{\gamma\gamma} \cdot F_\rho^2 = \sigma_{\gamma\gamma} \left( \frac{1}{1+Q^2/m_\rho^2} \right)^2 \quad (7)$$

Both the  $W$  dependence (formula 6) and the  $Q^2$  dependence of  $\sigma_t(Q^2, W)$  (formula 7) can also be derived from Vector Meson Dominance, VMD, (fig. 1b).

The  $Q^2$  dependence for  $W_{vis} < 3.5$  GeV and for  $W_{vis} > 3.5$  GeV is well consistent with the  $\rho$  pole as is demonstrated by the solid lines in figs. 4a and 4b which each have been normalized to the number of events in the plot. The statistics of our data is too poor to distinguish between the  $\rho$

pole and a more complicated series of vector mesons as suggested by general VMD.

We have further compared the expectation from VMD with the  $W$  dependence of our results. The solid line in fig. 3 is the expectation after folding in the detector resolution. Although at higher  $W_{\text{vis}}$  the agreement is good ( $\sigma_t = (1.21 \pm 0.13) \sigma_{\text{VMD}}$  (formula 7) for  $W_{\text{vis}} > 3.5$  GeV), the VMD curve can obviously not account for the increase at smaller  $W_{\text{vis}}$ . This we have already pointed out in our previous publication<sup>4</sup>.

We have extrapolated the data to  $Q^2=0$  using the  $\rho$  pole ansatz and corrected for the difference between  $W$  and  $W_{\text{vis}}$ . In doing that we have used the following ansatz for the hadronic cross section

$$\sigma_t(Q^2, W) = \left( A[240\text{nb} + 270\text{nbGeV}/W] + B/W^2 \right) F_\rho^2 \quad (8)$$

The best fit to the measured invariant mass distribution was achieved for  $A=0.97 \pm 0.16$  and  $B=2250 \pm 500$  nbGeV<sup>2</sup> with  $\chi^2/\text{df} = 0.5$ . This result is graphically represented by the hatched band in fig. 5 where we have plotted  $\sigma_{\gamma\gamma}$  versus the true invariant mass  $W$ . The limits represent the one standard deviation error of the fit.

It has been suggested<sup>11</sup> to include into the theoretical predictions non Regge terms like the quark box diagram (fig. 1c), the magnitude of which can be very roughly estimated by ( $q_i$  is the quark charge and  $m_q$  its mass)

$$\sigma_{\gamma\gamma}^{\text{quark}} = \frac{4\pi\alpha^2}{W^2} 3 \sum_i q_i^4 \ln(W^2/m_q^2) \quad (9)$$

The most important feature of this prediction is the  $1/W^2$  dependence. Including  $u$   $d$   $s$  quarks with masses of 100 MeV the magnitude of  $\sigma_{\gamma\gamma}^{\text{quark}}$  is 650 nb at  $W=1$  GeV. Note, that for small values of  $Q^2/W^2$  the  $Q^2$  dependence of the bare box diagram is given by  $1-2Q^2/W^2$  which is weaker than the  $\rho$  form factor. It is thus not certain if the deviations from VMD at small  $W$  can be explained quantitatively by a simple inclusion of the box diagram<sup>12</sup>

In conclusion we have measured for the first time hadron production in electron photon scattering for  $Q^2$  values up to 0.6 GeV<sup>2</sup> and over a wide range in  $W$ . The  $Q^2$  dependence is properly described by VMD in its simplest form ( $\rho$  pole). Above  $W_{\text{vis}} = 3.5$  GeV the data are well consistent with the VMD prediction whereas at smaller invariant masses a  $1/W^2$  term is needed which may qualitatively be understood as the contribution of point-like quarks.

#### Acknowledgements

We wish to thank Professors H.Schopper, G.Voss, E.Lohrmann and Dr.G.Söhngen for their valuable support. We are indebted to the PETRA machine group and the DESY computer center for their excellent performance during the experiment. We gratefully acknowledge the efforts



of all engineers and technicians of the collaborating institutions who have participated in the constructions and the maintenance of the apparatus.

## References

- 1) V.M.Budnev, I.F.Ginzburg, G.V.Meledin and V.G.Serbo,  
Phys.Rep. 15C(1975)182
- 2) C.Carimalo, P.Kessler and J.Parisi, Phys.Rev. D21(1980)669
- 3) S.J.Brodsky, T.Kinoshita and H.Terazawa, Phys.Rev. D4(1971)1532
- 4) PLUTO Collaboration, Ch.Berger et al., Phys.Lett. 89B(1979)120
- 5) J.H.Field Nucl.Phys. B168(1980)477
- 6) PLUTO Collaboration, Ch.Berger et al., Phys.Lett. 81B(1979)410
- 7) C.Bacci et al., Phys.Lett. 86B(1979)234
- 8) J.L.Siegrist Ph.D. thesis, SLAC-PUB-225(1980), UC-34d(1980)
- 9) A.Bäcker, Ph.D. thesis, Universität Siegen, Internal report  
DESY F33 77/03(1977)
- 10) T.F.Walsh, J.Physique C2 Suppl.3(1974)77  
S.J.Brodsky, same place, p.69  
J.L.Rosner in ISABELLE Physics Prospects,  
BNL report 17552(1972)316
- 11) M.Greco and Y.Srivastava, Nuovo Cimento 43A(1978)88  
S.J.Brodsky, F.E.Close and J.F.Gunion, Phys.Rev. D6(1972)177  
T.F.Walsh and P. Zerwas, Phys.Lett. 44B(1973)195
- 12) J.Gunion, Invited talk given at the International Workshop  
on Photon Photon Collisions, Amiens(1980),  
SLAC-PUB-2503(1980)

## Figure Captions

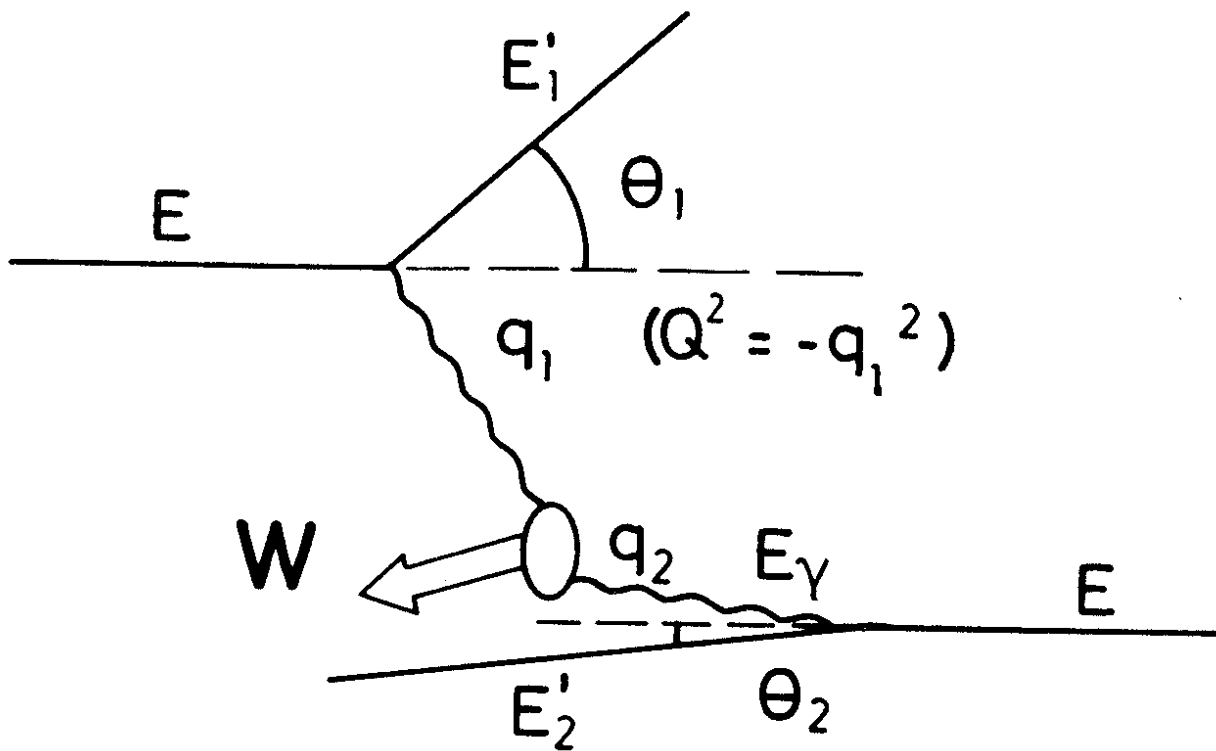
Fig. 1 a) Basic diagram for the reaction  $e^+e^- \rightarrow e^+e^- + \text{hadrons}$  with explanation of the kinematical symbols used in the text.  
b) Contribution of VMD to the total cross section  
c) Contribution of the free quark model to the total cross section

Fig. 2 Inclusive  $p_T^2$  distribution of the charged hadrons. The solid line is the prediction of the Monte Carlo simulation including the detector efficiency.

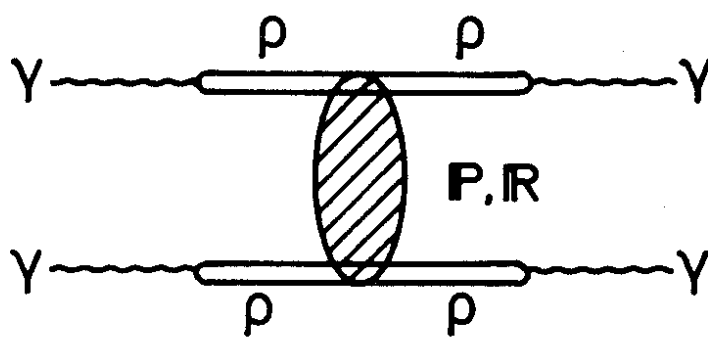
Fig. 3 The total cross section  $\sigma_t + \varepsilon\sigma_1$  at  $\langle Q^2 \rangle = 0.25 \text{ GeV}^2$  versus the visible invariant mass. The prediction of the VMD model is given by the solid line.

Fig. 4 The total cross section  $\sigma_t + \varepsilon\sigma_1$  as function of  $Q^2$  for  $W_{\text{vis}} < 3.5 \text{ GeV}$  (a) and for  $W_{\text{vis}} > 3.5 \text{ GeV}$  (b). The solid line is the prediction from  $\rho$  meson dominance.

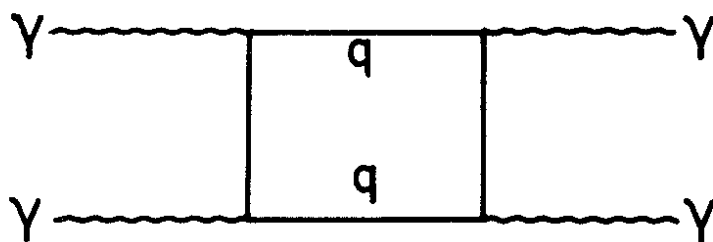
Fig. 5 The total photon photon cross section extrapolated to  $Q^2=0$ , versus the true invariant mass  $W$ . The hatched band represents the 1 std. limits as obtained from the fit. The VMD prediction is given by the dashed line.



a)



b)



c)

Fig 1

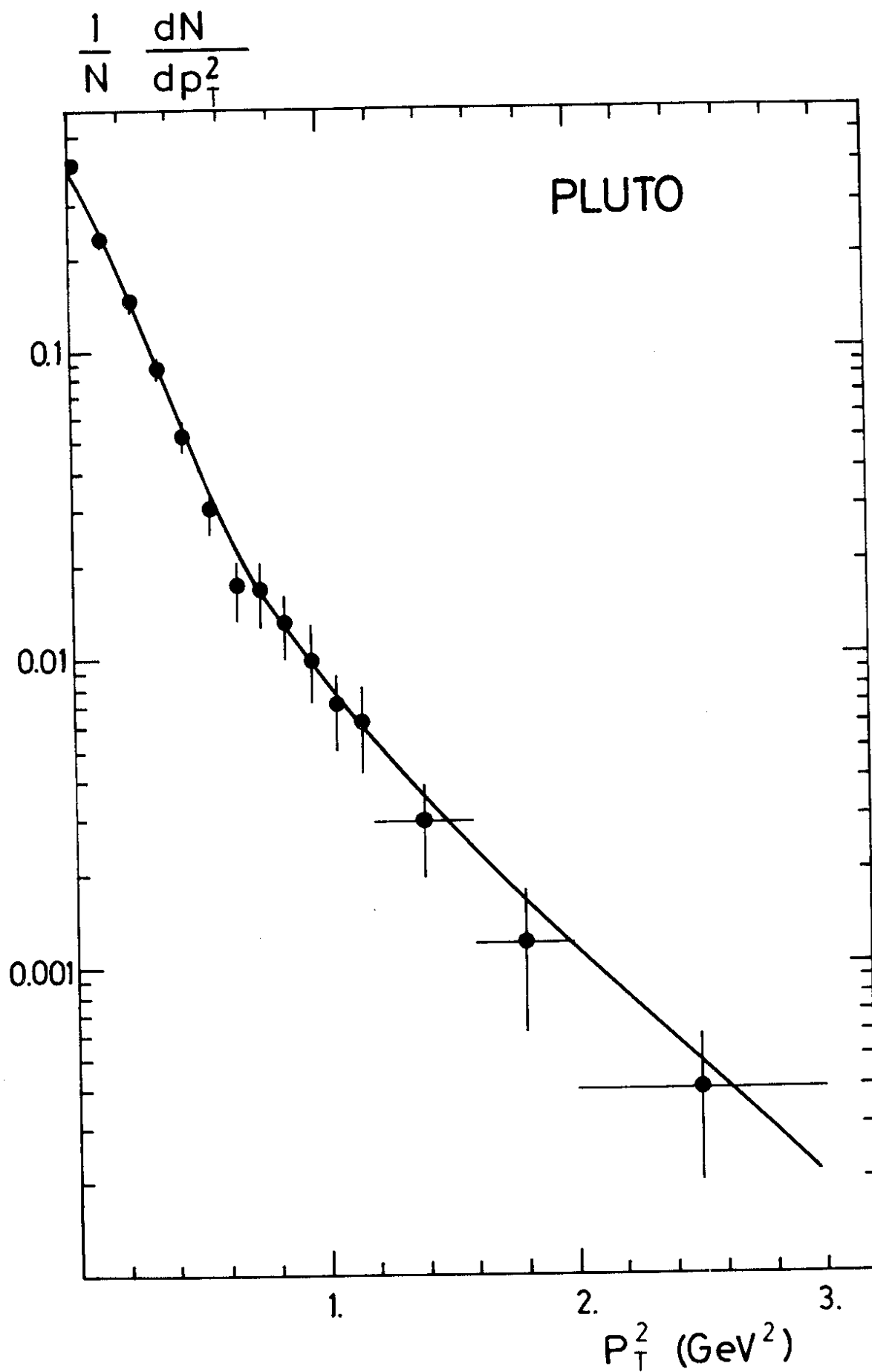


Fig 2

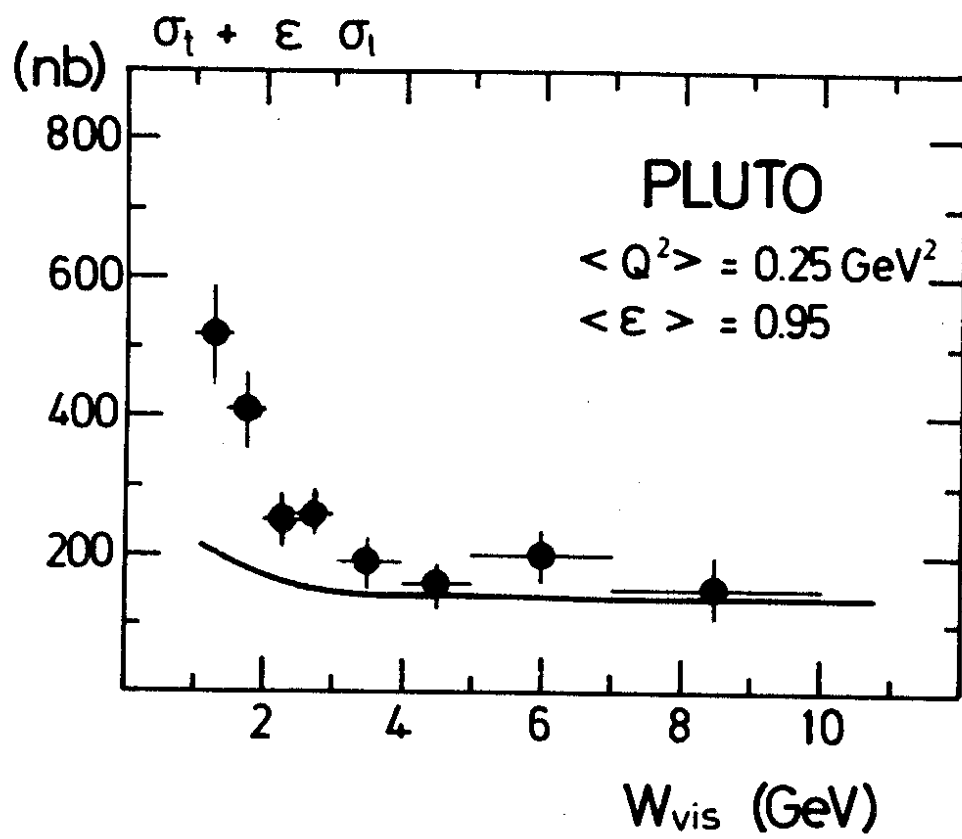


Fig 3

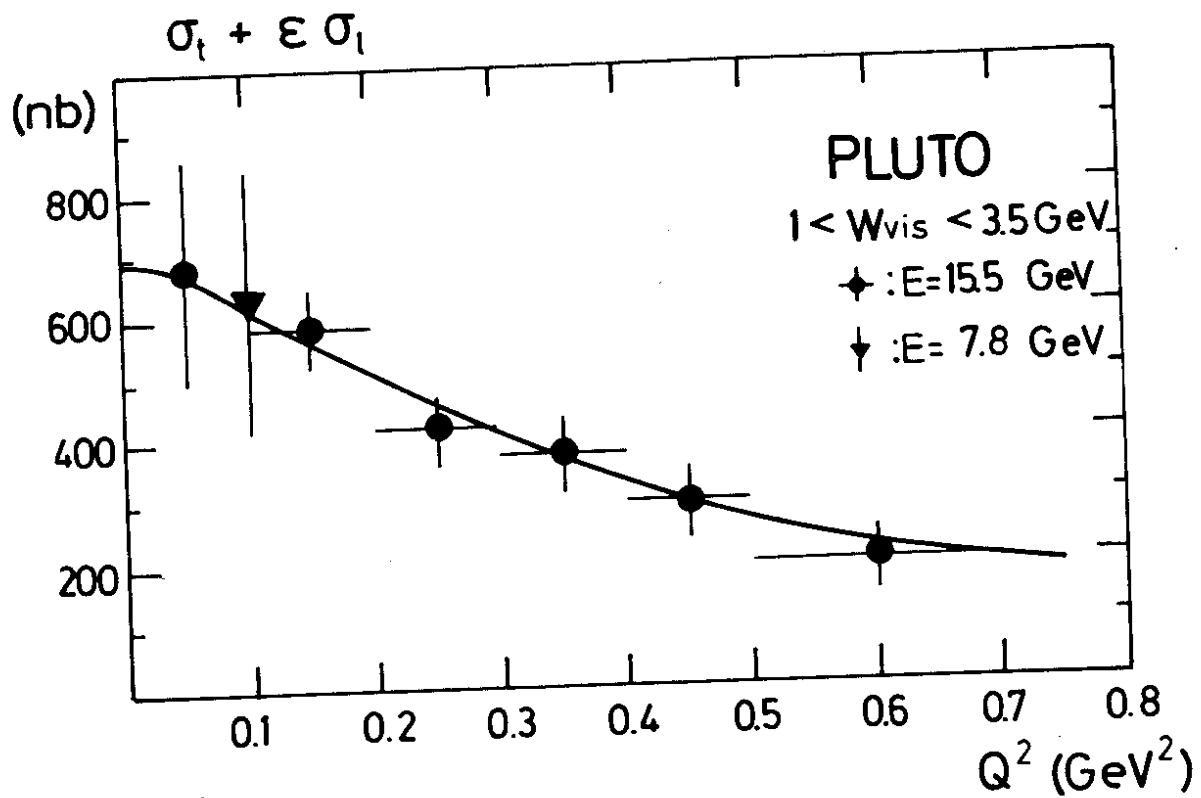


Fig 4a

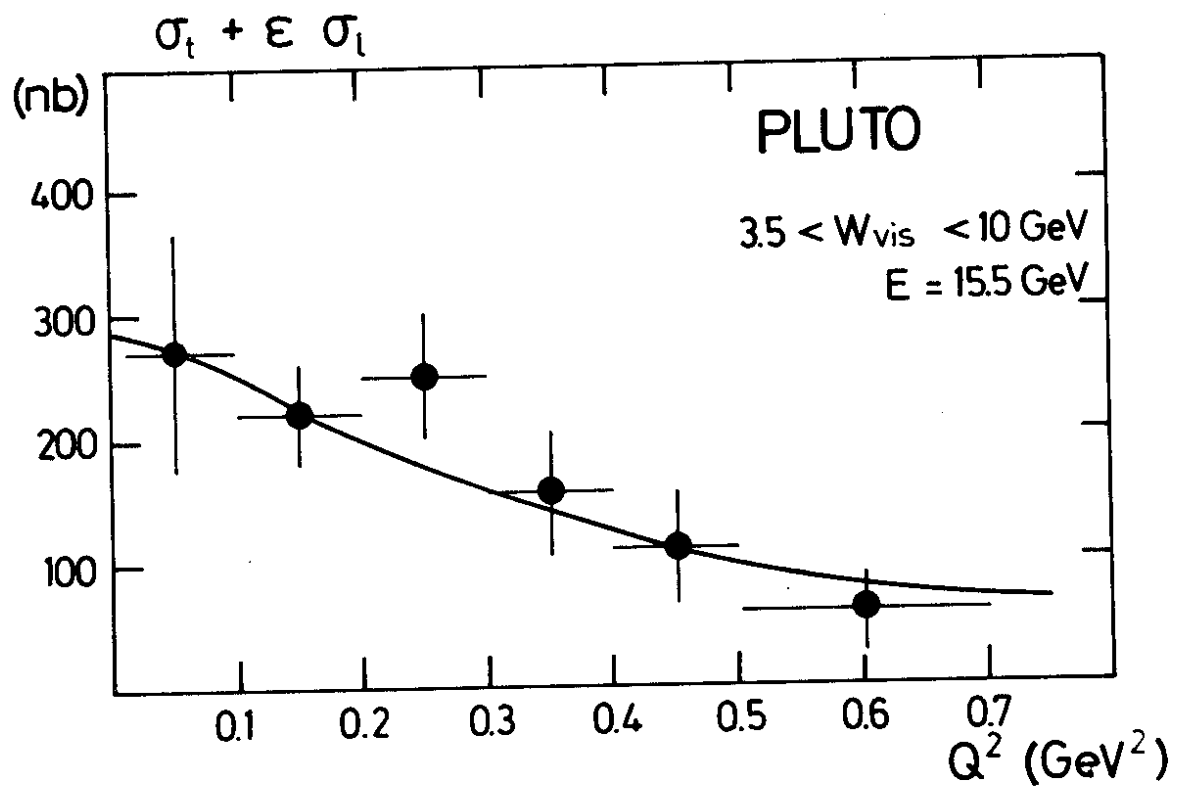


Fig 4b

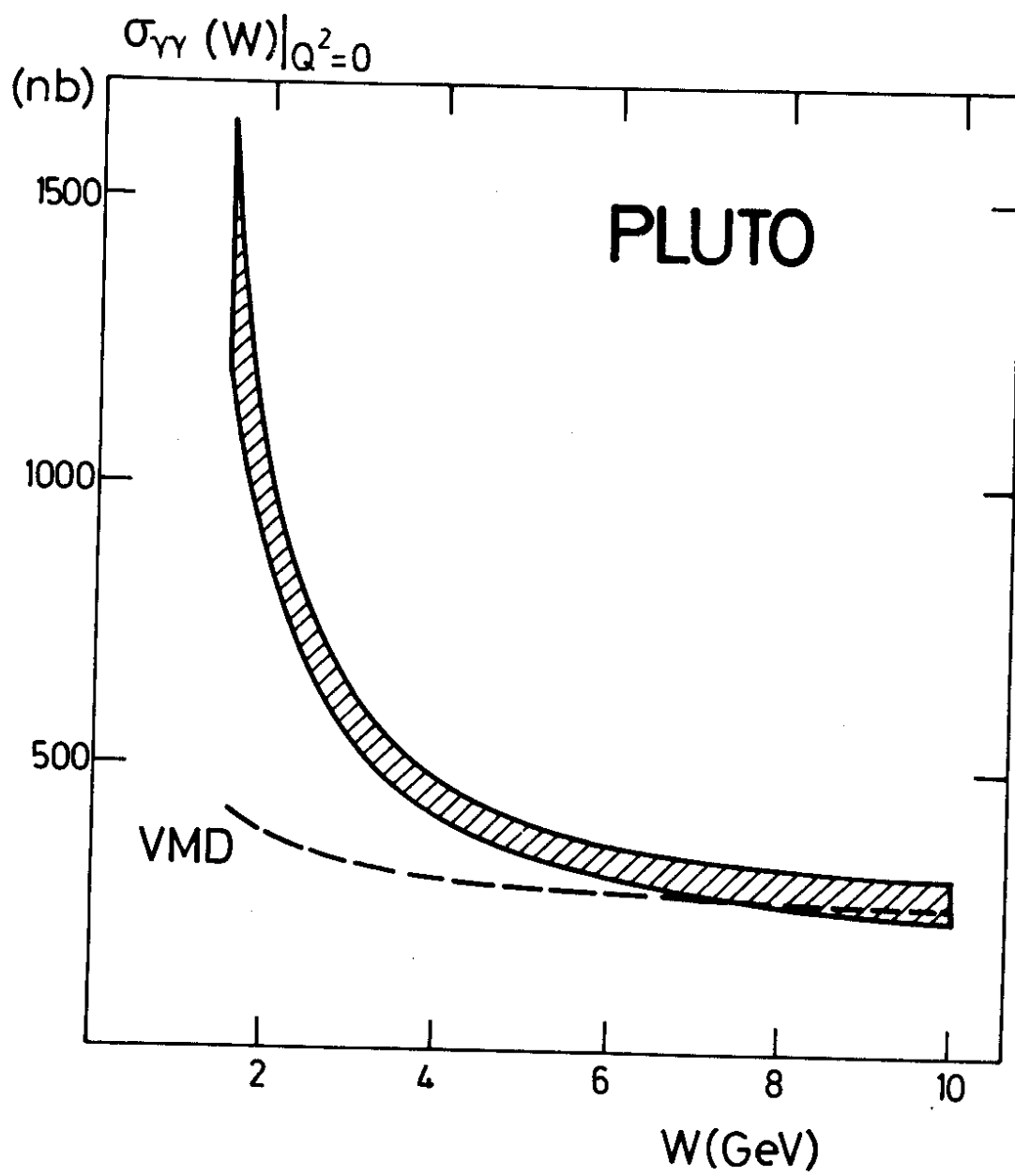


Fig 5